COOPERATIVE TIME-REVERSAL COMMUNICATION IN WIRELESS SENSOR NETWORKS

Richard J. Barton, Ji Chen, Kyle Huang, and Dagang Wu
Department of Electrical and Computer Engineering
University of Houston
Houston, TX 77205

ABSTRACT

In this paper, we study the feasibility of using a technique called *time reversal* for cooperative communication on wireless sensor networks. An indoor environment containing multiple wireless sensors is used as an example in which to test and demonstrate this approach. Using numerical simulations, we study the behavior of the peak power received at a target sensor as a function of the number of cooperating transmitting sensors as well as the level of transmitted signal distortion and timing synchronization errors. The simulation results demonstrate that time reversal is an effective generalization of beamforming that provides an efficient basis for cooperative communication on broadband multipath channels.

INTRODUCTION

In wireless sensor networks, integrated, low power sensors are widely utilized. Due to the power constraints imposed in such a deployment, energy efficient transfer of data becomes a critical issue. In situations where groups of sensors within the network are located in relatively close proximity, cooperative communication techniques are one possible solution to this problem [1]. In particular, if the point-to-point communication channels on the network are well modeled as frequency non-selective, distributed or cooperative beamforming has been proposed and studied [2]. For frequency-selective channels, beamforming itself is not generally appropriate, but a natural generalization of it, which we refer to as *time-reversal communication*, should still be effective. Time-reversal processing has been proposed and studied previously for other applications, including acoustical imaging [3], electromagnetic imaging [4], underwater acoustic communication [5], and very recently, for wireless communication channels [6-8]. In this paper, we study both the theoretical advantages and the feasibility of time reversal for cooperative communication in a wireless sensor network environment.

METHODOLOGY

The particular communication scenario we consider in this paper is Illustrated in Figures 1 and 2 below.

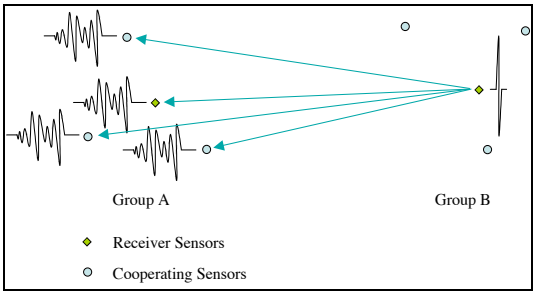

(a)

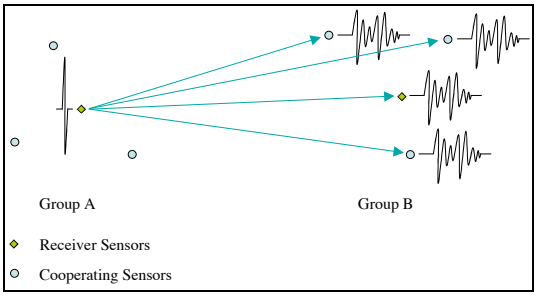

(b)

Figure 1. Training Phase: (a) Training for transmission from Group A to Group B, (b) Training for transmission from Group B to Group A.

We assume that there are two groups of sensors, A and B, such that the sensors in each group are in close proximity but the two groups are widely separated. To transmit information between the two groups, sensor a in group A is designated as the receiver for group A, and sensor b in group B is designated as the receiver for group B. During a training phase, sensor a transmits a short sequence of wide-band training pulses at relatively high power[1], which are

[1] In theory, the transmitted pulses should be sinc pulses with bandwidth greater than or equal to the bandwidth of the channel.

received at all of the sensors in group *B*. In turn, during a reciprocal training phase, sensor *b* transmits a similar sequence of training pulses which are received by all of the sensors in group *A*. We assume that each of the point-to-point paths on these two reciprocal channels is represented by an independent multipath channel with several resolvable paths, so that the received waveforms at all of the sensors are distorted in a different fashion. During each training phase, the receiving sensors independently perform *pulse estimation* in order to estimate the exact arrival time, duration, and shape of the received pulse.

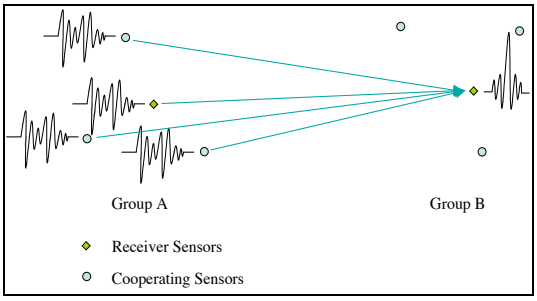

(a)

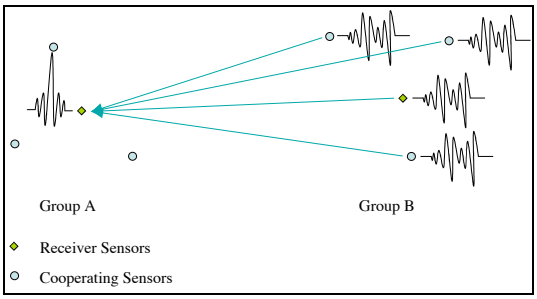

(b)

Figure 2. Transmission: (a) Group A to Group B, (b) Group B to Group A.

After the completion of the training phase, whenever group *A* wishes to transmit information to group *B*, all of the sensors in group *A* transmit the time-reverse of their estimated received waveforms modulated with the same data symbol in a synchronized, last-in-first-out fashion[2]. Similarly, whenever group *B* wishes to transmit information to group *A*, all of the sensors in group *B* transmit the time-reverse of their estimated received waveforms modulated with the same data symbol. Assuming the pulse estimation and transmission synchronization are performed perfectly, all of the transmitted waveforms from group *A* should recombine at sensor *b* to produce an impulsive waveform (equal to the sum of the autocorrelation functions of the various channel impulse responses) that maximizes the peak power output from the channel. Similarly, all of the transmitted waveforms from group *B* should recombine at sensor *a* to produce an impulsive waveform that again maximizes the peak power output from the channel. Hence, under perfect conditions, we expect to observe a waveform at the receiver node in each group with maximum possible peak output power that increases with the number of transmitting sensors.

In practice, of course, neither pulse estimation nor transmission synchronization will be perfect, and system performance will suffer as a result. To study the performance of the system, we vary the number of sensors per group and the assumed amount of signal distortion due to both pulse estimation and timing errors. We quantify the theoretically perfect performance as a function of the number of sensors as well as the degradation in performance due to pulse estimation and timing errors.

SIMULATION RESULTS

In this paper, we simulate the performance of the proposed cooperative communication technique in a virtual indoor laboratory environment. The signal propagation between sensors is simulated using an advanced electromagnetic propagation modeling method, the finite-difference time-domain (FDTD) method, which is capable of modeling arbitrary complex environments [9]. We performed simulations for a simple indoor environment comprising a single room with dimensions 3 meters by 2 meters by 2 meters. The dimensions were kept small to minimize the simulation time. The composition and electrical properties of the walls, ceiling, floor, and furnishings of the room are summarized in Table 1.

The geometry of the environment is illustrated in Figure 3. The environment contains a chair, a desk, and a bookshelf arranged as illustrated in the figure. In addition to the furniture, the room contains 10 sensors equipped with transceivers and omni-directional antennas arranged as illustrated in Figure 3. The sensor identified as the transmitter in Figure 3 corresponds to the target sensor for the cooperative transmission performed by the remaining sensors in the environment. We refer to it as the transmitter because it is the source of the original training pulse transmitted to the other sensors in the environment in order to estimate the distributed time-reversal waveforms transmitted cooperatively by the remaining sensors. As illustrated in Figure 3, the transmitter is located 1.8 meters above the floor, 5 of the sensors are located in a plane 1.5

In practice, any impulsive signal with sufficient bandwidth should work reasonably well.

[2] Here, we assume pulse-amplitude modulation is employed, and all of the sensors within a particular group share access to a common clock so that synchronized transmission is possible. There is no assumption of precise synchronization between the two groups.

meters above the floor, 3 more of the sensors are located in a plane 1.0 meters above the floor, and the single remaining sensor is located on the table at a height of 1.2 meters above the floor.

	Material	Relative Dielectric Constant	Conductivity (s/m)
Walls, Ceiling, Floor	Concrete	4.0	2.0×10^{-2}
Desk, Chair	Wood	1.5	0.0
Bookshelf	Metal	1.0	3.6×10^{7}

Table 1. Composition and electrical properties of simulated environment.

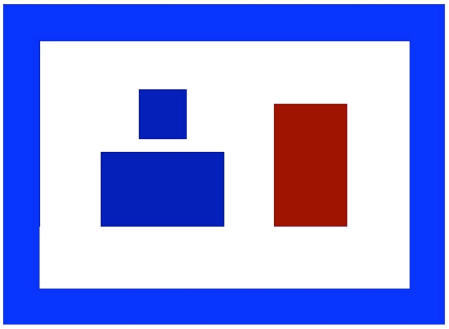

(a)

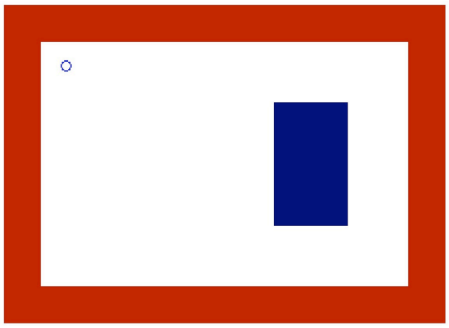

(b)

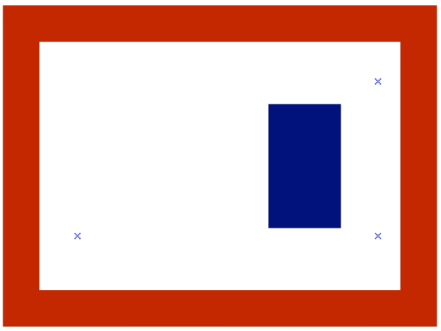

(c)

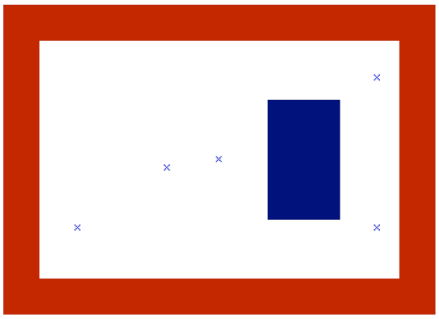

(d)

Figure 3. Geometry of simulated environment: (a) Overview with table and chair (blue) and bookshelf (red), (b) Cross-section at 1.8 meters with transmitter, (c) Cross-section at 1.0 meters with 3 sensors, (d) Cross-section at 1.5 meters with 5 sensors.

The transmitted training signal used for the simulations is illustrated in Figure 4. The signal is highly impulsive with a center frequency of about 1.5 GHz and a two-sided 10 dB bandwidth of approximately 800 MHz. Examples of the noise-free waveforms received at two different sensors corresponding to this transmitted training pulse are illustrated in Figure 5. As this figure indicates, the channel response varied noticeably from sensor to sensor. Finally, the waveform received back at the original transmitter corresponding to the synchronized retransmission of the time-reversed waveforms received at all of the sensors is illustrated in Figure 6. As expected, this waveform is nearly symmetric with a very sharp, well defined peak.

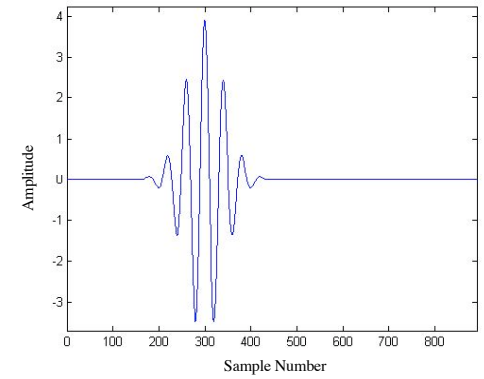

(a)

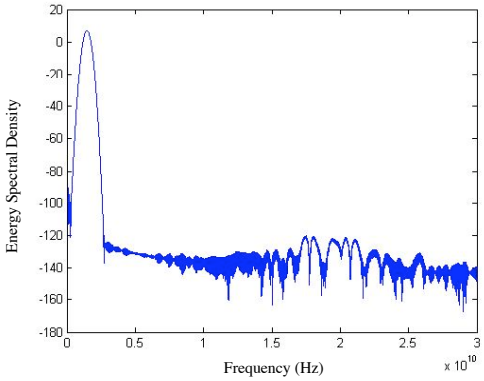

(b)

Figure 4. Transmitted training signal: (a) Time-domain waveform, (b) Energy spectrum.

The results of the simulation are summarized in Figures 7-9. The 3-D plots in Figure 7 illustrate the distribution of the peak power output from the received waveform in a 40-centimeter by 40-centimeter region centered at the original transmitter and confined to the same plane as the transmitter (1.8 meters above the floor.) As indicated, the maximum received peak power occurs at the original transmitter location in all cases regardless of the number of sensors cooperating in the retransmission; however, the shape of the peak power distribution clearly depends on the number of sensors cooperating. In particular, the received peak power decreases much more rapidly as a function of distance from the original transmitter location as the number of cooperating sensors increases. This is analogous to the narrowing of the beam pattern observed as the number of antenna nodes in a beam-forming array increases. Also, the distribution of received peak power is clearly not isotropic around the original transmitter location. In particular, there is a marked "axis of propagation" evident in all of the plots along which the received peak power decreases relatively slowly and in an oscillatory fashion. In the direction orthogonal to this axis of propagation, the rate of decrease in received peak power is much more rapid and more nearly monotonic. This behavior can be attributed to the fact that all transmitting sensors in this simulation are loosely clustered in the same half-plane on one side of the transmitter. The behavior would be more pronounced if the transmitting sensors were grouped more closely together and less pronounced if not all transmitter were located in the same half-plane.

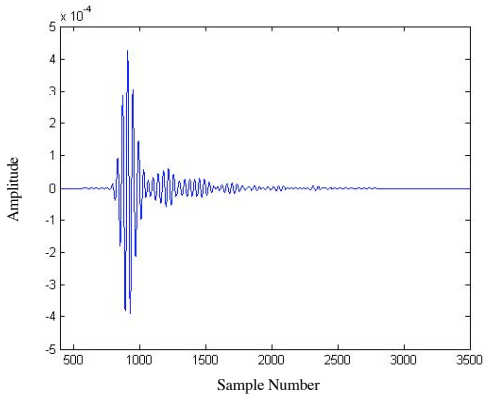

(a)

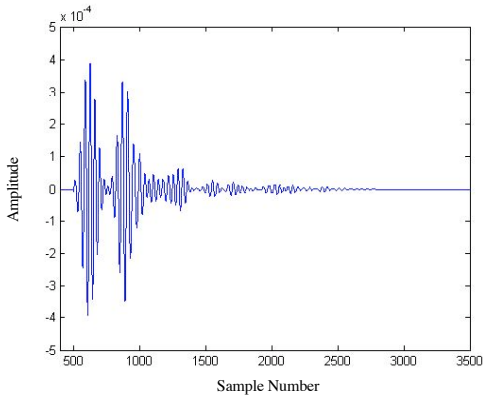

(b)

Figure 5. Received training waveforms at two different sensors: (a) Sensor 3, (b) Sensor 8.

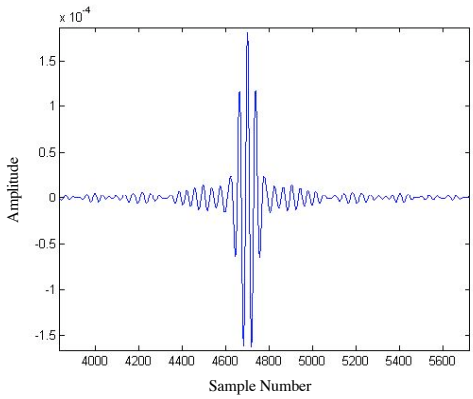

Figure 6. Received waveform from cooperative transmission by all sensors at original transmitter location.

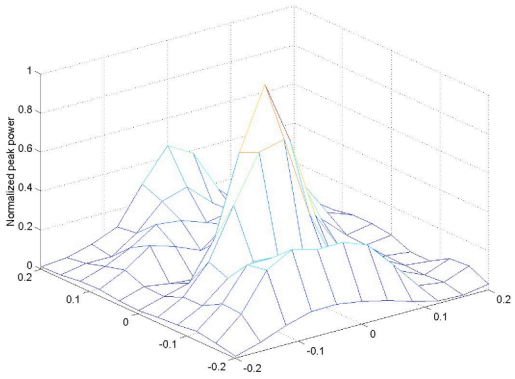

(a)

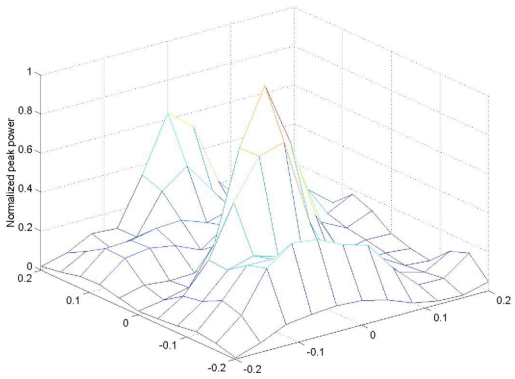

(b)

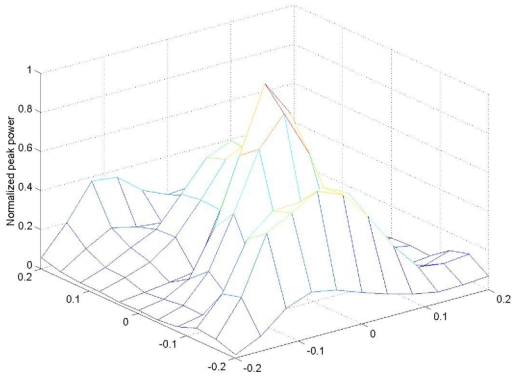

(c)

Figure 7. Received peak output power distribution near original transmitter location: (a) 9 Sensors, (b) 5 Sensors, (c) 3 Sensors.

Figure 8 illustrates the effects of pulse estimation and timing errors on the received peak power at the original transmitter location. To simulate the cumulative effects of both pulse estimation and timing errors, noise was added to the time-reversed waveforms prior to retransmission. The additive noise at each sensor was zero-mean, white, Gaussian, and independent from sensor to sensor. The results presented in Figure 8 are parameterized by signal-to-distortion ratio (SDR), which is calculated as the ratio of the energy in the noise-free training waveform received at each sensor divided by the variance of the i.i.d. noise samples added to distort the waveform. Prior to retransmission, the distorted waveform at each sensor was normalized to have unit energy.

The curves plotted in Figure 8 show the average peak power output from the channel at the original transmitter location for an ensemble of 100 independent transmissions from each sensor. As the figure indicates, the average peak output power increases monotonically as the SDR increases and attains a stable maximum value when the SDR increases above approximately 40 dB, which corresponds to nearly perfect pulse estimation and timing at each sensor. At the other extreme, the average peak output power attains a stable minimum value when the SDR drops below approximately 0 dB. At this point, the output from the channel corresponds essentially to transmitting only noise from each sensor. In the intermediate region, distortion in the retransmitted signal begins to cause a significant decrease in the peak power output from the channel when the SDR drops below 40 dB. The rate of decrease remains roughly linear on a log-log scale over the entire range of SDR values from 0 dB to 40 dB.

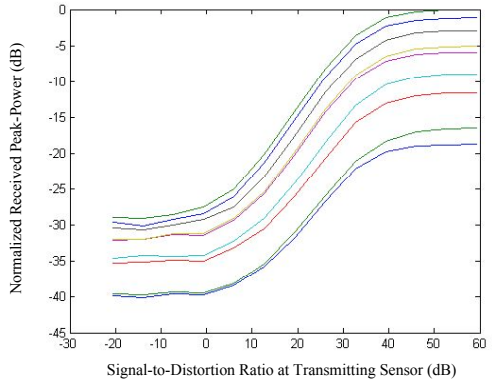

Figure 8. Cumulative peak output power vs. SDR for 1-9 transmitting sensors

Finally, Figure 9 depicts the rate of increase in average peak output power as a function of number of transmitting sensors for both very low (60 dB SDR) and very high (0 dB SDR) levels of distortion in the retransmitted signal. As the figure illustrates, the rate of increase in average peak output power is approximately linear for the very low SDR region and approximately quadratic in the very high SDR region. It is straightforward to show that this is the expected behavior for both cases.

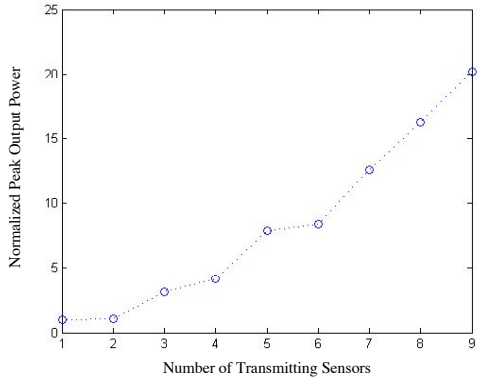

(a)

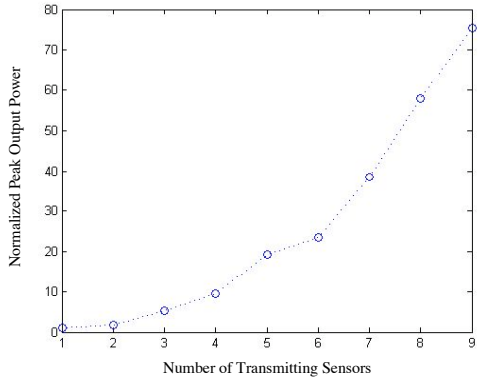

(b)

Figure 9. Growth rate of peak output power as a function of number of transmitting sensors: (a) Low SDR region, (b) High SDR region.

CONCLUSIONS

Cooperative time-reversal communication is a promising technique for transfer of information in low-power broadband sensor networks. It is particularly well suited for impulse radio networks since in that scenario, the waveform received at the original transmitter location corresponding to the retransmission of the time-reversed waveforms from all cooperating sensors can be shown to very nearly attain the maximum peak output power for the channel. That is, in that situation, the retransmitted time-reversed signal from each sensor corresponds to the signal that is "matched" to the channel, in the sense that the channel itself then plays the part of the optimal matched filter that would be implemented at the receiver if the channel were flat across the entire signal bandwidth.

REFERENCES

[1] A. Nosratinia, T. E. Hunter, and A. Hedayet, "Cooperative Communication in Wireless Networks," *IEEE Communications Magazine*, vol. 42, pp. 74-80, Oct., 2004.

[2] G. Barriac, R. Mudumbai, and U. Madhow, "Distributed Beamforming for Information Transfer in Sensor Networks," Proceedings of the Third International Symposium on Information Processing in Sensor Networks, 2004.

[3] P. Roux, A. Derode, A. Peyre, A. Tourin, and M. Fink, "Acoustical Imaging through a Multiple Scattering Medium Using a Time-Reversal Mirror," *Journal of the Acoustical Society of America*, vol. 107, no. 2, pp. L7-L12, Feb., 2000.

[4] A. B. Ruffin, J. Van Rudd, J. Decker, L. Sanchez-Palencia, L. Le Hors, J. F. Whitaker, and T. B. Norris, "Time Reversal Terahertz Imaging," *IEEE Journal of Quantum Electronics*, vol. 38, no. 8, pp. 1110-1119, August, 2002.

[5] G. F. EdelMann, W. S. Hodgkiss, S. Kim, W. A. Kupeman, and H. C. Song, "Underwater Acoustic Communication Using Time Reversal," Proceedings of the MST/IEEE OCEANS Conference and Exhibition, 2001.

[6] P. Kyritsi, G. Papanicolau, P. Eggers, and A. Oprea, "Miso Time Reversal and Delay-Spread Compression for Fwa Channels at 5 Ghz," *IEEE Antennas and Wireless Propagation Letters*, vol. 3, pp. 96-99, 2004.

[7] P. Kyritsi, G. Papanicolau, P. Eggers, and A. Oprea, "Time Reversal Techniques for Wireless Communications," Proceedings of the 60th Vehicular Technology Conference, 2004.

[8] T. Strohmer, M. Emami, J. Hansen, G. Papanicolau, and A. J. Paulraj, "Application of Time-Reversal with Mmse Equalizer to Uwb Communications," Proceedings of the Globecom 2004, 2004.

[9] A. Taflove, *Computational Electrodynamics: The Finite-Difference Time-Domain Method*. Norwood, MA: Artech House, 1995.